

DESIGN METHODS FOR WIDE-RANGE DIMMABLE FEEDBACK CONTROLLED ELECTRONIC BALLASTS

Mikhail Polonskii, Rafael A. Eichelberger, Thales M. Rodegheri, Jean C. A. Rigo, and Álysson R. Seidel

Department of Electric Engineering - FEAR – University of Passo Fundo

CEP 99001-970, C. P. 611/631, Passo Fundo – RS – Brazil

Phone +55.54. 3316-8229

E-mail: polonski@upf.br, arseidel@upf.br

Abstract – Dimmable electronic ballasts, used for fluorescent lamps feeding, reduce the electric power consumption and offer more lighting comfort. The dimming below of 30% of the rated lamp power, if the ballast is controlled in open loop, generally leads to the instable operation and, consequently, the extinguishing of the lamp arc. The article compares two resonant filter topologies in dimming operation, analyses dynamics of the frequency controlled dimmable electronic ballast and presents a practical approach to the closed-loop compensation. A dimmable ballast prototype was implemented in order to verify the proposed design method.

Keywords – design, electronic ballast, fluorescent lamp, and resonant filter.

I. INTRODUCTION

Dimmable electronic ballasts (DEB), used for fluorescent lamps (FL) feeding, reduce the electric power consumption and offer more lighting comfort. Wide-range frequency controlled DEB, which use switching frequency (f_s) variation to control the FL power, are the most popular and worldwide accepted. Usually, these DEB have two-stage structure, when the first one is a boost PFC and the second one is a half-bridge inverter. The two-stage structure, even more expensive in comparison with the single-stage one, is easier to design and allows controlling the inverter power switches with a duty cycle slightly less than 50%, avoiding this way the non linear electrophoresis phenomenon [1].

The DEB design involves two independent steps: 1) design of the PFC stage and 2) design of the resonant filter and half-bridge inverter stage. The PFC stage is usually a boost converter operating in CCM and controlled by an

integrated circuit (IC) like, for example, L6561 [2]. The half-bridge inverter feeds the FL through a LCC or CLC resonant filter, like shows Fig. 1, being these two filter topologies the most frequently used in commercially available DEB.

The half-bridge inverters, as shown in Fig. 1, count with the voltage mode filament heating circuit which include two secondary windings (L_2 and L_3) and two capacitors (C_f). This circuit is more appropriate in comparison with the filament heating provided by the C_p capacitor of the LCC filter because conditions one better FL filament power regulation in dimming operation [3]. The design of this circuit is out of the scope of the article.

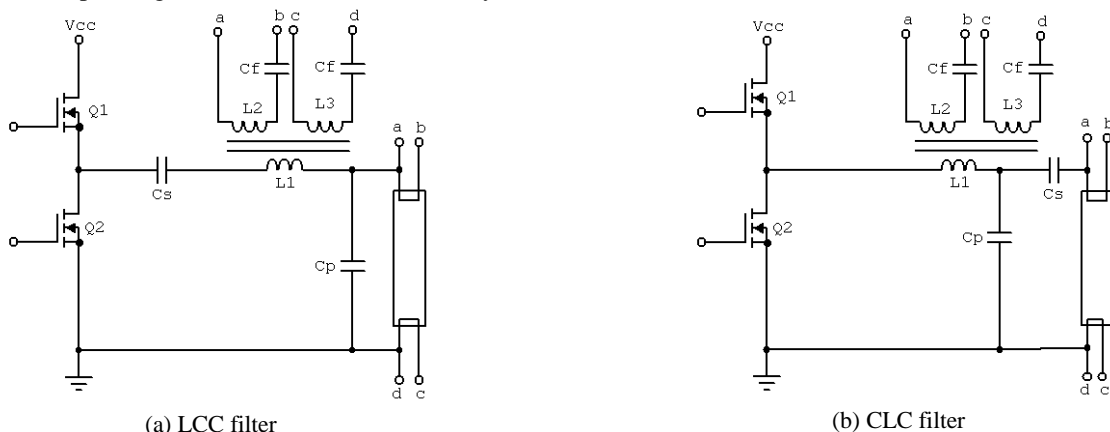
Topologies LCC and CLC, even include the same number of components, are not identical in terms of the resonant inductor current in dimming, being this difference investigated in Section II.

II. RESONANT FILTER DESIGN

There are two design procedures for LCC and CLC filter design proposed here.

A. LCC filter design

There are many ways to design LCC resonant filter like, for example, reported in [4], [5] and [6]. The design engineer still could use the “Ballast Designer” software, developed by International Rectifier [7], to design IR21592/21593-based DEB with the option to choose the configuration with one or two FL and the method of filaments heating. The main obstacle for an ample acceptance of this software is the impossibility for the user to define the mathematical model of the FL. Without this, the design is executed utilizing the FL mathematical models of the USA market which are not adjusted to the FL present in



(a) LCC filter

(b) CLC filter

Fig. 1. Half-bridge inverters, resonant filters and voltage mode filament heating circuit.

the Brazilian market, thus resulting in the situation when the DEB prototype or does not strike the FL or it strikes prematurely, that is, before the ending of the filament preheating interval. In this last case the FL remains in its rated power or until higher without entering in the dimming mode.

Here is proposed a LCC, see Fig. 1(a), filter design method integrated with a simulation procedure aiming the dimming curve and the inductor current calculations. The procedure calculates for a chosen number of odd harmonics. The design method is as following:

Step 1: Define FL model, CC bus voltage (V_{CC}) and the lowest switching frequency ($f_{S,MIN}$). Here is used a Philips TLD T8/32W FL, single lamp configuration, $V_{CC}=400$ V, $f_{S,MIN} = 50$ kHz.

Step 2: Obtain a mathematical model of the FL. Here is used the exponential model reported in [8] which defines the FL equivalent resistance R as the function of the FL power P as

$$R(P) = 4013 \cdot e^{-0,074 \cdot P} + 9447 \cdot e^{-0,332 \cdot P} \quad (1)$$

A look-up table-based FL model can be used too.

Step 3: Choose the resonant frequency of the L_I - C_P circuit.

Step 4: Choose a C_S value.

Step 5: Calculate a L_I value utilizing the numerical values of C_S , f_{RES} , V_{CC} , $f_{S,MIN}$ and the FL rated power. First, an approximated value L_{SS} of L_I is calculated supposing the capacitance of C_S infinite [9]. For this (2) is used.

$$\left(\frac{V_S}{V_o}\right)^2 = (1 - \Omega^2)^2 + \left(\frac{\Omega}{Q_P}\right)^2 \quad (2)$$

where $Q_P = R/(\omega_o L_{SS})$; $\Omega = \omega/\omega_o$; ω_o is the resonant frequency of the L_{SS} - C_P circuit; $V_S = \frac{2V_{CC}}{\pi}$ is the amplitude of the fundamental harmonic of the inverter output voltage ($0.5 \cdot V_{CC}$); V_o stands for the FL voltage; $\omega = 2\pi f_{S,MIN}$. This way, L_{SS} is determined as:

$$L_{SS} = \frac{R}{\omega} \cdot \sqrt{\left(\frac{V_S}{V_o}\right)^2 - (1 - \Omega^2)^2} \quad (3)$$

Using L_{SS} , the value of C_P is calculated:

$$C_P = \frac{1}{\omega_o \cdot L_{SS}} \quad (4)$$

Using (5), see [9]

$$V_o = \frac{V_S}{\sqrt{\left(\frac{C_P + C_S}{C_S} - \omega^2 \cdot L_I \cdot C_P\right)^2 + \left(\frac{1}{\omega \cdot C_S \cdot R} - \frac{\omega \cdot L_I}{R}\right)^2}} \quad (5)$$

and introducing the auxiliary variable A, B and C, the exact value of L_I is calculated:

$$A = \omega^4 \cdot C_P^2 + \frac{\omega^2}{R^2} \quad (6)$$

$$B = \frac{2 \cdot (C_S + C_P) \cdot C_P \cdot \omega^2}{C_S} - \frac{2}{R^2 \cdot C_S} \quad (7)$$

$$C = \left(\frac{C_S + C_P}{C_S}\right)^2 + \frac{1}{(\omega \cdot R \cdot C_S)^2} - \frac{V_S^2}{2 \cdot R \cdot P} \quad (8)$$

Finally, L_I is calculated resolving the following equation:

$$A \cdot L_I^2 + B \cdot L_I + C = 0 \quad (9)$$

Generally, resolving (9), one positive and one negative root are obtained, and the positive one should be selected for the resonant inductor implementation.

B. CLC filter design

The CLC resonant filter transfer function $V_o(s)/V_S(s)$ (Fig.1(b)) is

$$\frac{V_o(s)}{V_S(s)} = \frac{C_S \cdot R \cdot s}{L_I \cdot C_P \cdot C_S \cdot R \cdot s^3 + L_I \cdot (C_P + C_S) \cdot s^2 + R \cdot C_S \cdot s + 1} \quad (10)$$

where s is the Laplace transformation variable. The filter has three parameters which should be chosen in such a way that at $f_{S,MIN}$ the FL power is the rating one. The filter design is based on the assumption that the value of C_S , which is many times larger of what C_P , little influences the dimming curve and the phase angle of the resonant inductor current at $f_{S,MIN}$. The auxiliary variables a , b , c and d are:

$$a = (C_S + C_P) \cdot \omega^2 \quad (11)$$

$$b = R \cdot C_S \cdot \omega \quad (12)$$

$$d = C_P \cdot C_S \cdot R \cdot \omega^3 \quad (13)$$

$$e = \left(V_S \cdot C_S \cdot \omega \cdot \sqrt{\frac{R}{2P}}\right)^2 \quad (14)$$

Finally, the following equation defines the L_I value:

$$(a^2 + d^2) \cdot L_I^2 + (-2a - 2 \cdot b \cdot d) \cdot L_I + (1 + b^2 - e) = 0 \quad (15)$$

The positive root should be chosen for L_I .

III. DIMMING CURVE

The dimming curve $P(f_S)$ permits to evaluate the switching frequency sweep related to the EMI problems. Here, the proposed numeric algorithm plots the dimming curve on the base of the FL model, V_{CC} and the resonant filter transfer function. The algorithm, implemented in MATLAB, is depicted on Table 1.

TABLE I
 $P(f_S)$ calculation algorithm

Define: V_{CC} , FL model, $f_{S,MIN}$
Initial Loop:
Choose: C_P , C_S
Calculate: L_I
Calculate: the L_I current phase at $f_S = f_{S,MIN}$
Repeat Initial Loop ? <i>if</i> not break ;
End of Initial Loop
Frequency Loop:
Increment f_S ;
<i>if</i> $f_S > f_{S,MAX}$ break ;
Power Loop:
$P = P + corr$;
$R = R(P)$;
Calculate: I_{LAMP} , V_{LAMP}
$PP = I_{LAMP} \cdot V_{LAMP}$;
<i>if</i> $(PP - P) < 0.05$ break ;
$corr = 0.5 \cdot (PP - P)$;
End of Power Loop
Calculate: amplitude (I_{MAX}) and phase (PHASE) of L_I current;
Calculate: RMS value (I_{RMS}) of L_I current;
End of Frequency Loop
Plot: $P(f_S)$, $I_{MAX}(f_S)$, $I_{RMS}(f_S)$, $PHASE(f_S)$

The developed simulation program made possible to obtain various dimming curves for LCC and CLC filters, as shown in Fig. 2(a) and (b). Fig. 3 shows peak and RMS resonant inductor currents for LCC and CLC topologies.

Resonant filter should be optimized to minimize the resonant inductor current phase, aiming the reduction of the reactive power circulating in the half-bridge inverter, however it is difficult to say which resonant filter structure, LCC or CLC, is preferable. This should be a topic for futures investigations.

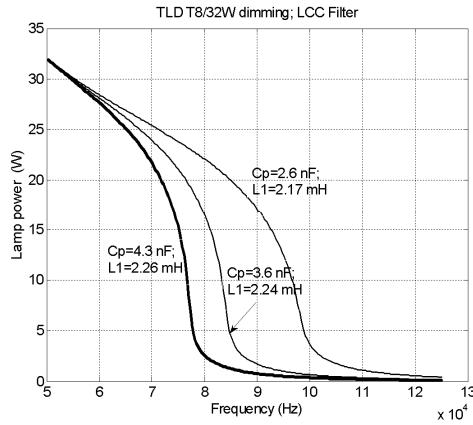
Fig. 4 shows the resonant CLC inductor current phase and the f_s sweep at $P=0,02 \cdot P_{NOM}$ as the functions of C_p capacitor variation.

Analyzing Fig. 4, one can conclude that some insignificant phase reduction of phase can be obtained by diminishing of the C_p value, however this cause the f_s sweep to grow, which possibly aggravates the EMI problem. Almost equal results were obtained for the LCC filter.

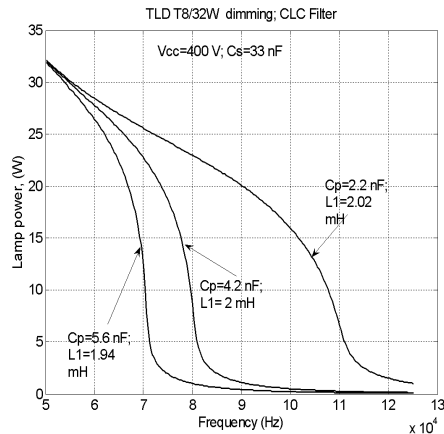
This way, a more detailed analysis should be performed aiming resonant filter optimization.

IV. STABILITY ANALYSIS AND COMPENSATION

Stable operation of LF in the wide range (3% to 100%) dimming applications can be obtained under the closed-loop control [10]. Here only the dimming by switching frequency variation is analyzed since that the Section I includes the dimming methods comparison.

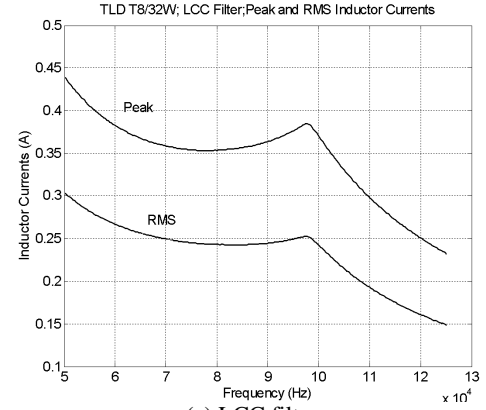


(a) LCC filter

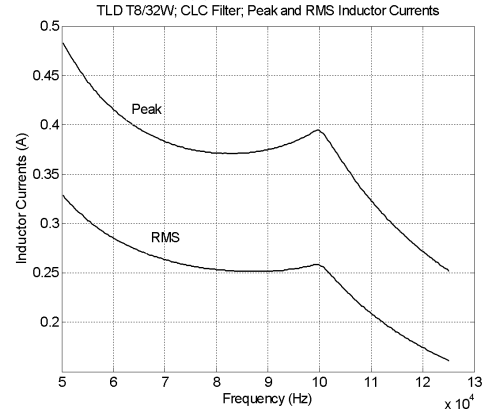


(b) CLC filter

Fig. 2. Dimming curves.

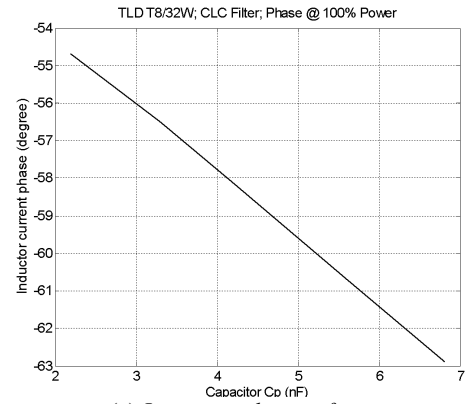


(a) LCC filter

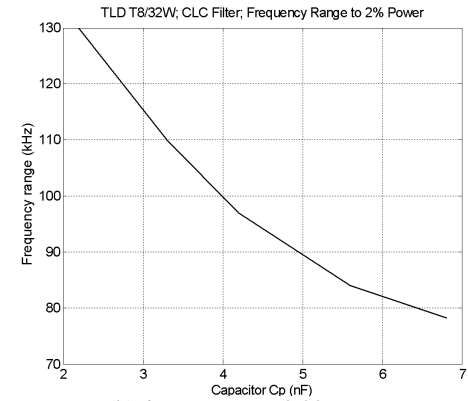


(b) CLC filter

Fig. 3. Resonant inductor RMS and Peak currents.



(a) L_f current phase at $f_{s, MIN}$



(b) f_s sweep at $P=0,02 \cdot P_{NOM}$

Fig. 4. L_f current phase at $f_{s, MIN}$ (a) and $f_{s, MAX}$ sweep at $P=0,02 \cdot P_{NOM}$ (b)

In the accordance with [11], the FL incremental impedance appears as a phase shift between the FL voltage envelope and the FL current one and can be modeled by the 1st order liner model. The model presents a pole on the left half-plane and a zero on the right half-plane and was analyzed in details in [12]. Analytical tools, proposed in [10], permit to derive a 6th order liner model for a 2nd order resonant filter and are useful for dynamic analysis of frequency-controlled DEB, however are very complex.

A practical approach to the stability analysis, used here, utilizes the frequency response of the DEB controlled in open-loop. The frequency response is obtained in the form of Bode graphs, the method widely adopted for linear systems analysis [13]. Although the FL is not a linear system, a linearization in turn of some operating point is possible. Fig. 5 depicts the diagram used to obtain the Bode graphs.

The $V_{in}(t)$ voltage is:

$$V_{in}(t) = V_{OFFSET} + A \cdot \sin(2 \cdot \pi \cdot \omega_{MOD}) \quad (16)$$

The magnitude of V_{OFFSET} determines the dimming level of the FL, because the frequency on the VCO (Voltage Controlled Oscillator) output is proportional to the voltage on its input. To obtain the frequency response, the FL power was adjusted to 7 W. Fig. 6 shows the Bode graphs obtained for FL TLD T8/32W model, $V_{CC}=400$ V; $L_I=2$ mH; $C_S=220$ nF; $C_P=4.2$ nF.

To achieve stable closed-loop operation, a DEB should include a compensator aiming sufficient gain and phase

margins. A compensator should include one integrator to avoid stable-state error, thus way a PI compensator is a viable choice. Experiments proved that the gain crossover frequency of 7000 Hz is sufficient for stable arc control.

Observing Fig. 6, one can conclude that the compensator corner frequency of about 1000 Hz guarantees a phase margin of about 50°. By the following procedure one can easily design the PI compensator:

$$1) \omega_c = 1000 \cdot 2 \cdot \pi = 6280 \frac{rad}{s} \quad (17)$$

where ω_c is the PI compensator's corner frequency.

2) The compensator gain should be equal to 15 dB at ω_c to guarantee the gain crossover frequency of 7000 Hz. This way, the compensator gain is:

$$20 \cdot \log_{10} \left(\frac{k}{\omega_c} \right) = 15 dB \quad (18)$$

$$k = 10^{\frac{15}{20}} \cdot \omega_c = 35333 \quad (19)$$

3) Finally, the PI compensator transfer function is:

$$G_C(s) = k \cdot \frac{\left(\frac{1}{\omega_c} \cdot s + 1 \right)}{s} = \frac{5.626 \cdot s + 35333}{s} \quad (20)$$

This transfer function can be easily implemented by one operational amplifier.

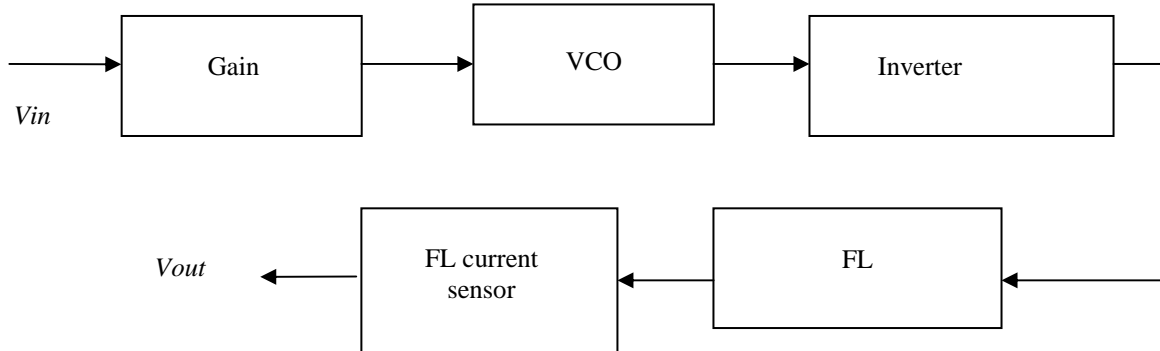


Fig. 5. Diagram of the frequency response measuring.

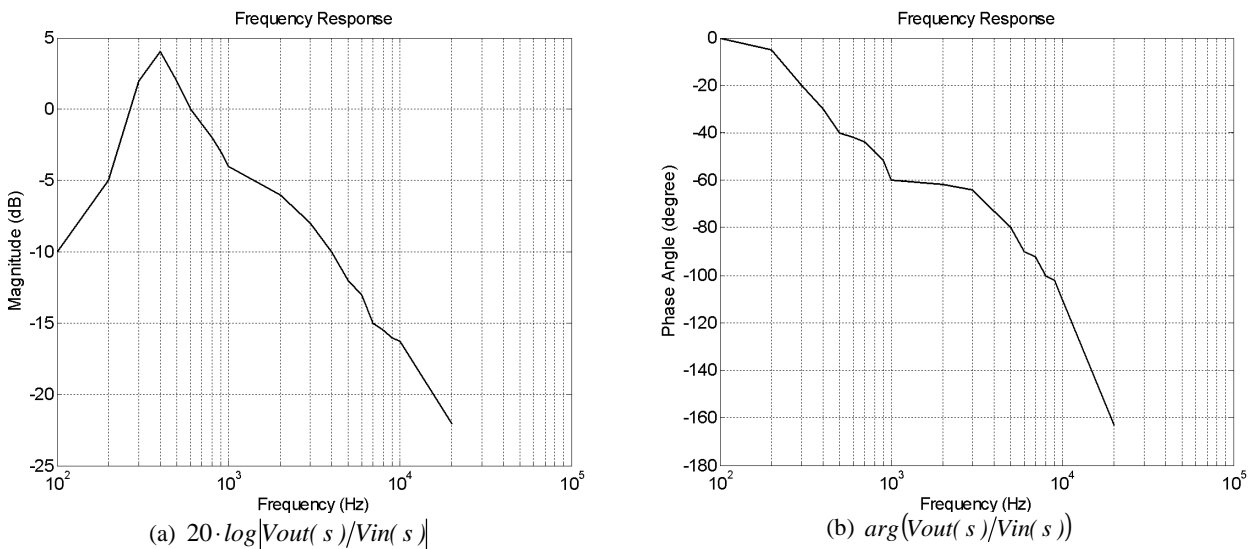


Fig. 6. Frequency response measured on the open-loop controlled prototype.

V. EXPERIMENTAL RESULTS

To verify the proposed analysis, a DEB prototype has been established on the base of IR21592 and LM324 operational amplifier. The CLC filter has been implemented as following: LCC resonant filter $L_f = 2$ mH; $C_p = 4.2$ nF; $C_s = 220$ nF. A L6561-based PFC supplied 400 V bus. Fig. 7 shows the measured input and FL currents.

VI. CONCLUSION

The paper presents a design method for wide dimming range electronic ballasts. The method permits to calculate the resonant filter parameters, to plot dimming curve and to obtain the inductor RMS and peak currents variations in dimming. Closed-loop control permits a stable FL dimming until low power levels. A practical approach used for the stability analysis permits to design a PI compensator for stable closed-loop operation. A DEB prototype, based on the proposed design method, operates stably while the FL is dimming till 3% of its rated power. Any attempt to dim the FL below 30% of its rated power under open-loop control results in arc distinguishing.

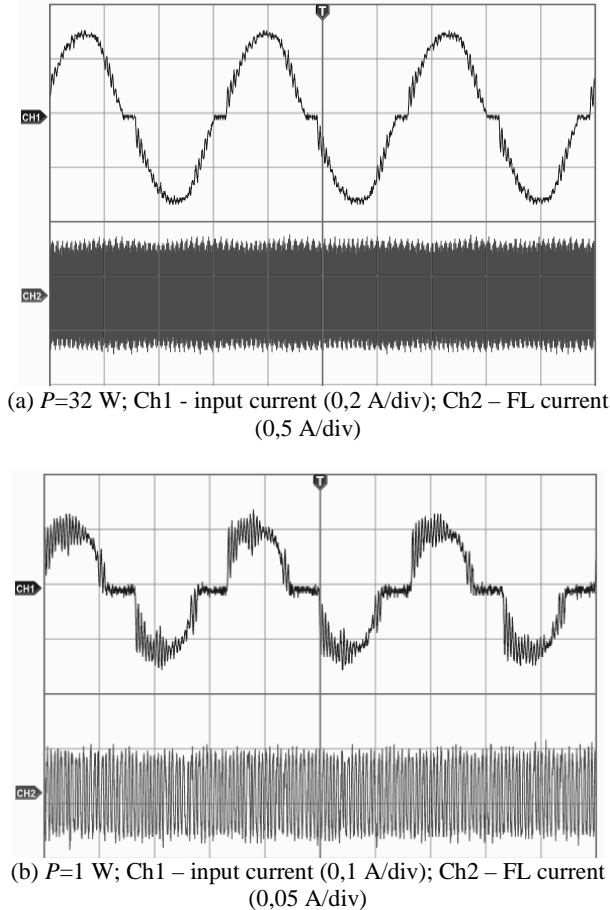


Fig. 7. Experimentally measured currents.

VII. ACKNOWLEDGMENT

The authors are grateful of CNPq for the financial support of this work.

REFERENCES

- [1] F. Raizer, "Problems with lamp current control using a PWM signal". *IEEE Industry Application Magazine*, pp. 54-59. November/December 2002.
- [2] ST Microelectronics. "Electronic Ballast with PFC, using L6574 e L6561". Application Note AN 993. 2000.
- [3] L. H. Goud, J. W. F. Dorleijn, "Standardized data for Dimming of Fluorescent Lamps" in *Proc. of IEEE IAS*, v.1, pp. 673-679, 2002.
- [4] Perdigão M. Electronic Ballast Investigation. Master of Science Thesis. University of Coimbra. Portugal. 2004 (in Portuguese).
- [5] C. Moo, H. Cheng, H. Chen, H. Yen, "Designing Dimmable Electronic Ballast with Frequency Control", " in *Proc. of IEEE Applied Power Electronics Conference*, pp. 727-733, 1999.
- [6] M. Kazimierczuk, W. Szaraniec, "Electronic Ballast for Fluorescent Lamps", *IEEE Trans. on Power Electronics*, v. 8, n.4, Oct. 1993, pp.386-395.
- [7] International Rectifier. Ballast Designer. Access: <http://www.irf.com/whats-new/nr051026.html>
- [8] M. Cervi, Á. R. Seidel, F. E. Bisogno, R. N. do Prado, "Fluorescent Lamp Model Based on the Equivalent Resistance Variation." in *Proc. of IEEE 37th Industry Applications Society Annual Meeting*, 2002, Pittsburg. IAS, 2002. v. 1. p. 680-684.
- [9] Power Electronics Handbook. Ed. M. Rashid. Academic Press. 1192 p., 2006.
- [10] Y. Yin, R. Zane, J. Glaser, R.W. Erickson, "Small-Signal Analysis of Frequency-Controlled Electronic Ballasts." *IEEE Trans. on Circuits and Systems -I*, v. 50, n.8, Aug. 2003, p.1103-1110.
- [11] E. Deng, I. Negative Incremental Impedance of Fluorescent Lamps. Ph. D. Thesis. California Institute of Technology, 1996, p.133.
- [12] S. Ben-Yakov, M. Shvartsas, S. Glozman, "Statics and Dynamics of Fluorescent Lamps Operating at High Frequency: Modeling and Simulation." *IEEE Trans. on Industry Electronics*, v.38, n.6, Nov./Dec. 2002, p.1486-1492.
- [13] K. Ogata, "Engenharia de Controle Moderno." 4 ed. São Paulo: Pearson. 2003, p. 788 (in Portuguese).